Analytica Chimica Acta 853 (2015) 514–520

Contents lists available at ScienceDirect

Analytica Chimica Acta

journal homepage: www.elsevier.com/locate/aca

Visualizing tributyltin (TBT) in bacterial aggregates by specific rhodamine-based fluorescent probes

Xilang Jin [a,1], Likai Hao [b,1], Mengyao She [a], Martin Obst [b], Andreas Kappler [b], Bing Yin [a,c], Ping Liu [a], Jianli Li [a,*], Lanying Wang [a], Zhen Shi [a]

[a] Ministry of Education Key Laboratory of Synthetic and Natural Functional Molecule Chemistry, College of Chemistry & Materials Science, Northwest University, Xi'an, Shaanxi 710069, PR China
[b] Center for Applied Geosciences Eberhard Karls University Tübingen, Hölderlinstr. 12, 72074 Tübingen, Germany
[c] College of Chemistry, Beijing Normal University, No. 19, Xinjiekouwai Street, Haidian District, Beijing 100875, PR China

HIGHLIGHTS

- Six novel rhodamine-based probes for TBT were designed, synthesized and tested.
- The probes show high selectivity and sensitivity in the range from 6 to 20 mM of TBT.
- The probe was used to map TBT in cell-EPS-mineral aggregates.
- Here we present the first examples of fluorescent probes for microscopic TBT imaging.

GRAPHICAL ABSTRACT

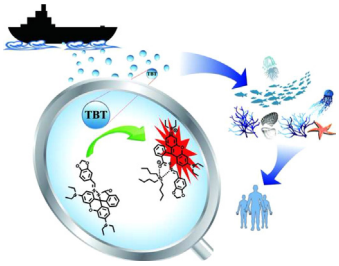

ARTICLE INFO

Article history:
Received 20 January 2014
Received in revised form 26 September 2014
Accepted 6 October 2014
Available online 13 October 2014

Keywords:
Fluorescent probes
Tributyltin (TBT)
Rhodamine
Fluorescence imaging
Mapping TBT distribution

ABSTRACT

Here we present the first examples of fluorescent and colorimetric probes for microscopic TBT imaging. The fluorescent probes are highly selective and sensitive to TBT and have successfully been applied for imaging of TBT in bacterial *Rhodobacter ferrooxidans* sp. strain SW2 cell-EPS-mineral aggregates and in cell suspensions of the marine cyanobacterium *Synechococcus* PCC 7002 by using confocal laser scanning microscopy.

1. Introduction

The coastal areas represent the most important areas of the oceans from a human perspective. There are hundreds of new chemicals introduced into coastal environments every year [1,2]. The marine antifouling paint additive tributyltin (TBT), which is one of the most toxic substances ever deliberately put into the sea is ubiquitous in aquatic organisms and marine systems and represents a major environmental problem [3]. Organotin compounds accumulate in marine sediments and marine organisms such as fish, shellfish and squids [4]. The consumption of contaminated marine species leads to human dietary exposure [5], and generates DBT (dibutyltindichloride, Sn(*n*-butyl)$_2^{2+}$), a

* Corresponding author. Tel.: +86 029 88302604; fax: +86 029 88302601.
E-mail addresses: lijianli@nwu.edu.cn, chem311@nwu.edu.cn (J. Li).
[1] These authors contributed equally to this work.

http://dx.doi.org/10.1016/j.aca.2014.10.005
0003-2670/

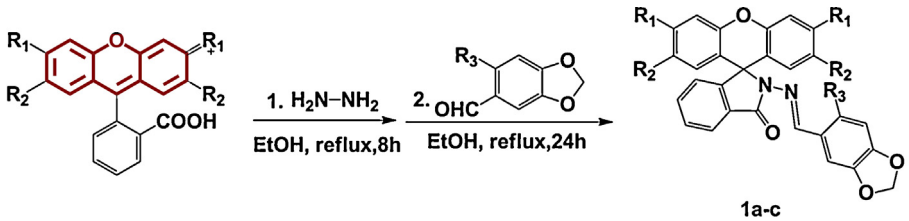

1a: R_1 = NEt_2, R_2 =H, R_3 = H; 1b: R_1 = NEt_2, R_2 =H, R_3 = Br; 1c: R_1 = NEt_2, R_2 =H, R_3 = NO_2;
2a: R_1 = NHEt, R_2 = CH_3, R_3 = H; 2b: R_1 = NHEt, R_2 = CH_3, R_3 = Br; 2c: R_1 = NHEt, R_2 = CH_3, R_3 = NO_2;
3a: R_1 = OH, R_2 =H, R_3 = H; 3b: R_1 = OH, R_2 =H, R_3 = Br; 3c: R_1 = OH, R_2 =H, R_3 = NO_2;

Scheme 1. Structures of probes **1**–**3**.

metabolite of tributyltin that is detectable in the human liver. TBT degrading bacteria and TBT-resistant microorganisms have been reported in polluted river water and coastal seawater [6,7]. Although extensive research about TBT interactions with microorganisms has been performed in the last decades [8], the underlying mechanisms for these interactions are still unknown. Thus, direct evidence for TBT bioaccumulation or transformation from in situ (confocal) fluorescence microscopic images is needed to increase our knowledge of the underlying mechanisms.

Therefore, the goal of this study was to develop a new fluorescent TBT probe that is able to systematically monitor TBT in environmental samples and to analyze the distribution of TBT in and around TBT-resistant and TBT-degrading bacteria. Among various metal-specific fluorophores, rhodamine-based dyes have attracted considerable interest. Thus, rhodamines are widely used as fluorescent probes and molecular markers in chemistry and biological research [9–13]. A variety of fluorescent molecular probes for the detection of Cu^{2+} [14–16], Zn^{2+} [17,18], Hg^{2+} [19,20] with high sensitivity and selectivity have been developed in recent years. Surprisingly, no probe has been reported which could be used for the specific detection of TBT. Here we present several novel fluorescent probes that could specifically label TBT.

Specifically, we provide the design and synthesis of nine novel Schiff-base probes (Scheme 1) which were synthesized from rhodamine B, rhodamine 6G and fluorescein by a two-step procedure. The structures were verified by X-ray crystallography, ^{1}H NMR, ^{13}C NMR spectra and mass spectrometry data. We believe that the probes represent significant breakthroughs for visualizing TBT. Moreover, these probes also provide a potential approach to study native microbial TBT resistance and degradation.

2. Experimental

2.1. Instrumentation

Fluorescence spectra were measured on a Hitachi F-4500 fluorescence spectrophotometer equipped with a xenon discharge lamp, in a 1 cm quartz cell. The high-resolution mass spectrum (HRMS) were measured using a Bruker microTOF-Q II ESI-Q-TOF LC/MS/MS spectrometer by means of the electronic spray ionization (ESI). NMR spectra were recorded on a Varian INOVA-400 MHz spectrometer (at 400 MHz for ^{1}H NMR and 100 MHz for ^{13}C NMR) using tetramethylsilane (TMS) as internal standard. X-ray crystallography data were collected on a Bruker Smart APEX II CCD diffractometer. The fluorescence images were obtained by Leica SPE confocal laser scanning microscope equipped with an ACS APO 63*x* water immersion lens (NA = 1.15).

2.2. Chemicals and reagents

Rhodamine B, rhodamine 6G, fluorescein, hydrazine hydrate (80%) and piperonyl aldehyde were all obtained from J&K Chemical Co., Beijing, China. The butyltin derivatives (monobutyltin, dibutyltin, tributyltin, monophenyltin, diphenyltin, triphenyltin) were all obtained from Sigma–Aldrich Co., Shanghai, China. Unless otherwise noted, all the other materials used in these experiments were purchased from Sinopharm Chemical Reagent Beijing Co., Beijing, China. Analytical thin layer chromatography was performed using Merck 60 GF254 silica gel (pre-coated sheets, 0.25 mm thickness). The solutions of various testing species were prepared from $CrCl_3$, $CuCl_2$, $NiCl_2$, $CdCl_2$, $HgCl_2$, $MnCl_2$, $PbCl_2$, $CaCl_2$,

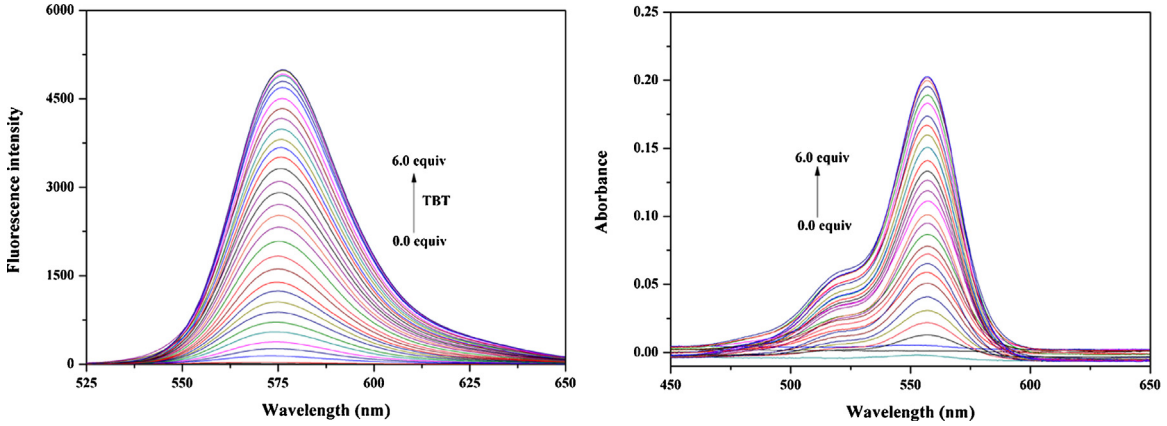

Fig. 1. Fluorescence intensity (λ_{ex} = 510 nm) (a) and absorption (b) changes of probe **1a** (5 μM) upon addition of TBT (0.0–6.0 equiv.) in CH_3CN–PBS (1/99, v/v, pH 7.4) solution. *Inset*: calibration curve of fluorescence intensity (λ_{ex} = 510 nm) (a) and absorption (b) in dependence of TBT concentrations. The fluorescence intensity was measured at 577 nm. The absorbance was measured at 558 nm.

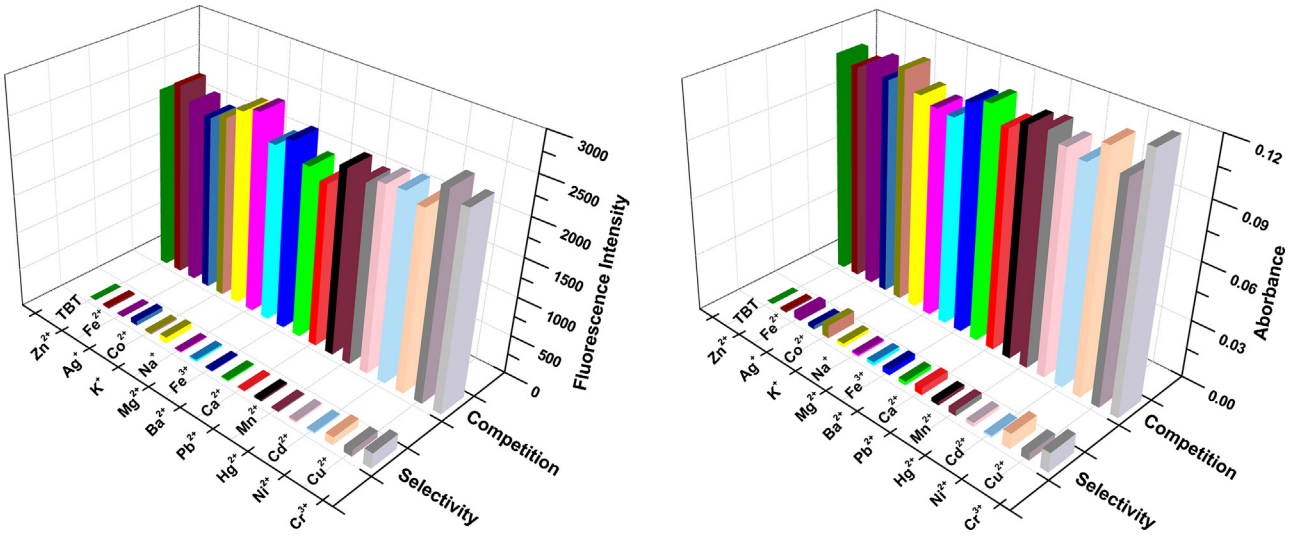

Fig. 2. Fluorescence intensity (a) and absorption (b) changes of probe **1a** (5 μM) upon the addition of various metal ions (30 μM) with and without the presence of TBT (10 μM) in CH_3CN–PBS (1/99, v/v, pH 7.4) solution. Black bars represent the fluorescence response of **1a** to the metal ions of interest. (1) Cr^{3+}; (2) Cu^{2+}; (3) Ni^{2+}; (4) Cd^{2+}; (5) Hg^{2+}; (6) Mn^{2+}; (7) Pb^{2+}; (8) Ca^{2+}; (9) Ba^{2+}; (10) Fe^{3+}; (11) Mg^{2+}; (12) Na^{+}; (13) K^{+}; (14) Co^{2+}; (15) Ag^{+}; (16) Fe^{2+}; (17) Zn^{2+}; (18) TBT. The colored bars represent the subsequent addition of 10 μM TBT to the respective solutions. The fluorescence intensity was measured at 577 nm. The absorbance was measured at 558 nm. (For interpretation of the references to color in this figure legend, the reader is referred to the web version of this article.)

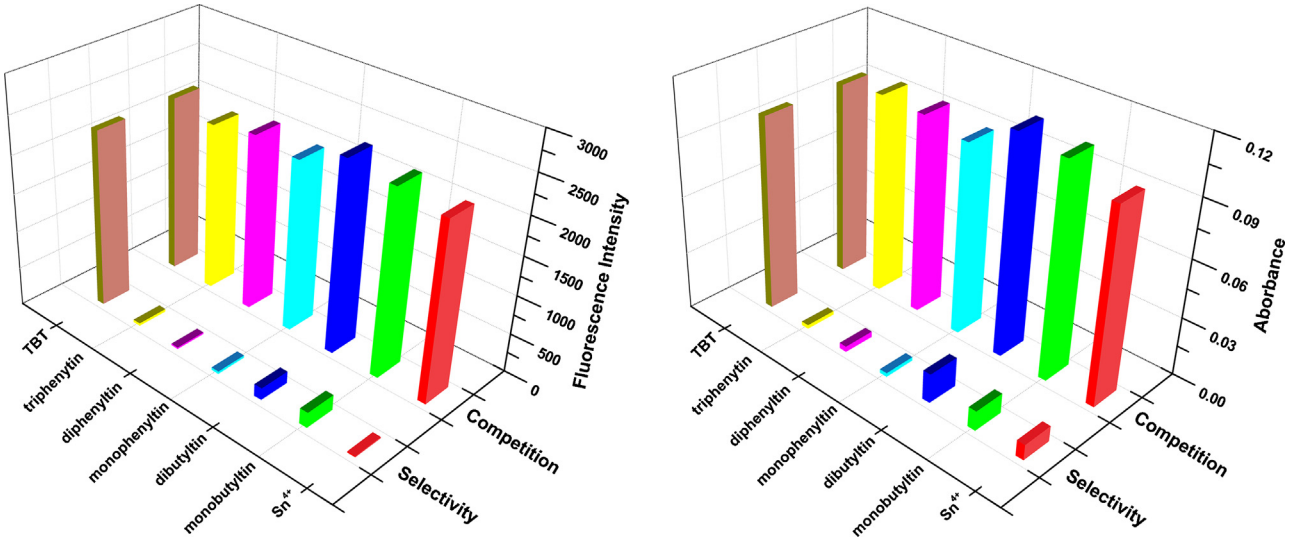

Fig. 3. Fluorescence intensity (a) and absorption (b) changes of probe **1a** (5 μM) upon the addition of various metal ions (30 μM) with and without the presence of TBT (10 μM) in CH_3CN–PBS (1/99, v/v, pH 7.4) solution. Black bars represent the fluorescence response of **1a** to the metal ions of interest. (1) Sn^{4+}; (2) monobutyltin; (3) dibutyiltin; (4) monophenyltin; (5) diphenyltin; (6) triiphenyltin; (7) TBT. The colored bars represent the subsequent addition of 10 μM TBT to the respective solutions. The fluorescence intensity was measured at 577 nm. The absorbance was measured at 558 nm. (For interpretation of the references to color in this figure legend, the reader is referred to the web version of this article.)

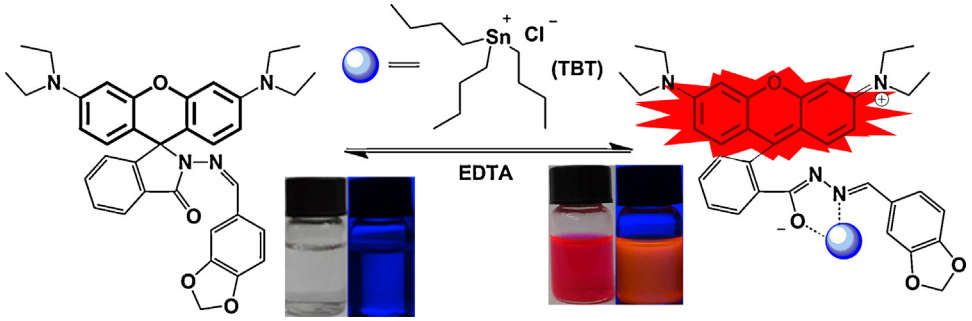

Scheme 2. The TBT-sensing mechanism of compound **1a**.

$$f_{(r)}^{+} = \left(\frac{\partial\rho(\vec{r})}{\partial N}\right)_{\upsilon} = \left(\rho(r)_{N+1} - \rho(r)_{N}\right)_{\upsilon} \quad (1a)$$

$$f_{X}^{+} = q_{X}^{N+1} - q_{X}^{N} \quad (1b)$$

Scheme 3. Where N is the number of electrons, υ is the external potential, qX is the electronic population of atom X in a molecule.

$BaCl_2$, $FeCl_3$, $MgCl_2$, NaCl, KCl, $CoCl_2$, $AgNO_3$, $FeCl_2$, $ZnCl_2$, respectively. Double distilled water was used throughout the study.

2.3. General procedure fluorescence analysis

Probes **1a** stock solution (500 μM) was prepared in acetonitrile. The solutions of various testing species stock solutions (500 μM) were prepared in distilled water. For the titration experiments, different amounts of TBT and 0.10 mL of 500 μM probes were mixed and filled up with PBS to 10 mL in volumetric tubes. For the interference experiments, 15 μM TBT, 0.10 mL of 500 μM probe **1a** and 0.60 mL of 500 μM testing species were mixed and filled up with PBS to 10 mL in volumetric tubes. 1 mL aliquots were pipetted into a 1 cm cuvette for spectral measurements. 5 nm bandpasses were used for both excitation and emission wavelengths. Excitation wavelengths of 510 (for probe **1a**–**c**) and 480 (for probe **2a**–**c**) nm were used for the acquisition of emission spectra.

2.4. Cell culture and fluorescence imaging

Cells of the photosynthetic Fe(II)-oxidizing *Rhodobacter* sp. strain SW2 [21] and of the marine cyanobacterium *Synechococcus* PCC 7002 [22] were cultured as described elsewhere. Aggregates of the cultures were incubated with probe **1a** (50 μM) for 1 h in the dark. Aliquots were placed on glass-slides, covered with coverslips, sealed to prevent them from drying and analyzed using a Leica SPE confocal laser scanning microscope equipped with a 63*x* water immersion lens (NA = 1.15).

The cyanobacterial strain *Syncechococcus* PCC 7002 shows autofluorescence when excited with the 561 nm laser that was also used for the TBT probe **1a**. However, the emission spectra are sufficiently different for an unambiguous differentiation of probe **1a** signal (566–596 nm) from autofluorescence signal starting approximately at 600 nm for the concentrations used in this study.

Table 1
Spectroscopic properties of the probes[a] for TBT.

Probe	$\lambda_{ex,max}$(nm)	$\lambda_{em,max}$(nm)	Φ^{b}(%)	τ(ns)
1a	558	577	0.78	2.50
1b	558	574	0.32	2.68
1c	559	576	0.45	2.37
2a	531	554	0.85	3.15
2b	532	557	0.52	3.80
2c	533	556	0.25	3.69

[a] All spectroscopic measurements were performed in CH_3CN- PBS (1/99, v/v, pH 7.4) solution at room temperature.
[b] Reported quantum yields are based on rhodamine B, Φ = 0.97 in ethanol.

2.5. Synthesis of compounds *1*–*3*

The synthesis of compounds **1**–**3** is shown in the Supporting information.

3. Results and discussion

3.1. Spectroscopic properties

We evaluated the spectral properties and TBT responses of the probes in CH_3CN–PBS(1/99, v/v, pH 7.4, PBS: Phosphate Buffered Saline) solution. Only probes **1a**–**c** and **2a**–**c** showed high selectivity and sensitivity to TBT in solution. The spectroscopic properties of the probes **1a**–**c** and **2a**–**c** are summarized in Table 1. Although probes **1a**–**c** and **2a**–**c** all may function as fluorescent chemosensors for TBT, we found that probes **1b**–**c** and **2b**–**c** are inferior to probe **1a** and **2a** in terms of reactivity. Thus, only probe **1a** was chosen for further studies that are presented here and

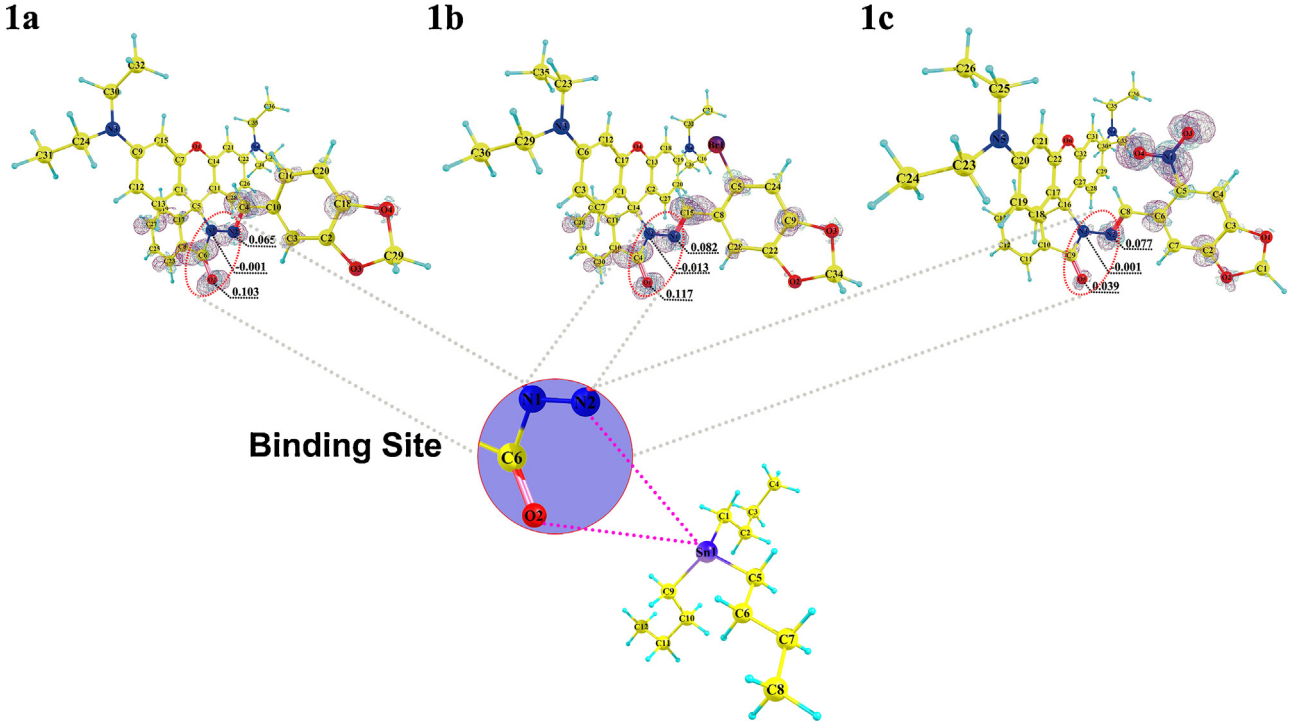

Fig. 4. The 3D representation and condensed Fukui function $f^{+}(r)$ of the iso-value of 0.003 a.u. (positive in red color and negative in green color). (For interpretation of the references to color in this figure legend, the reader is referred to the web version of this article.)

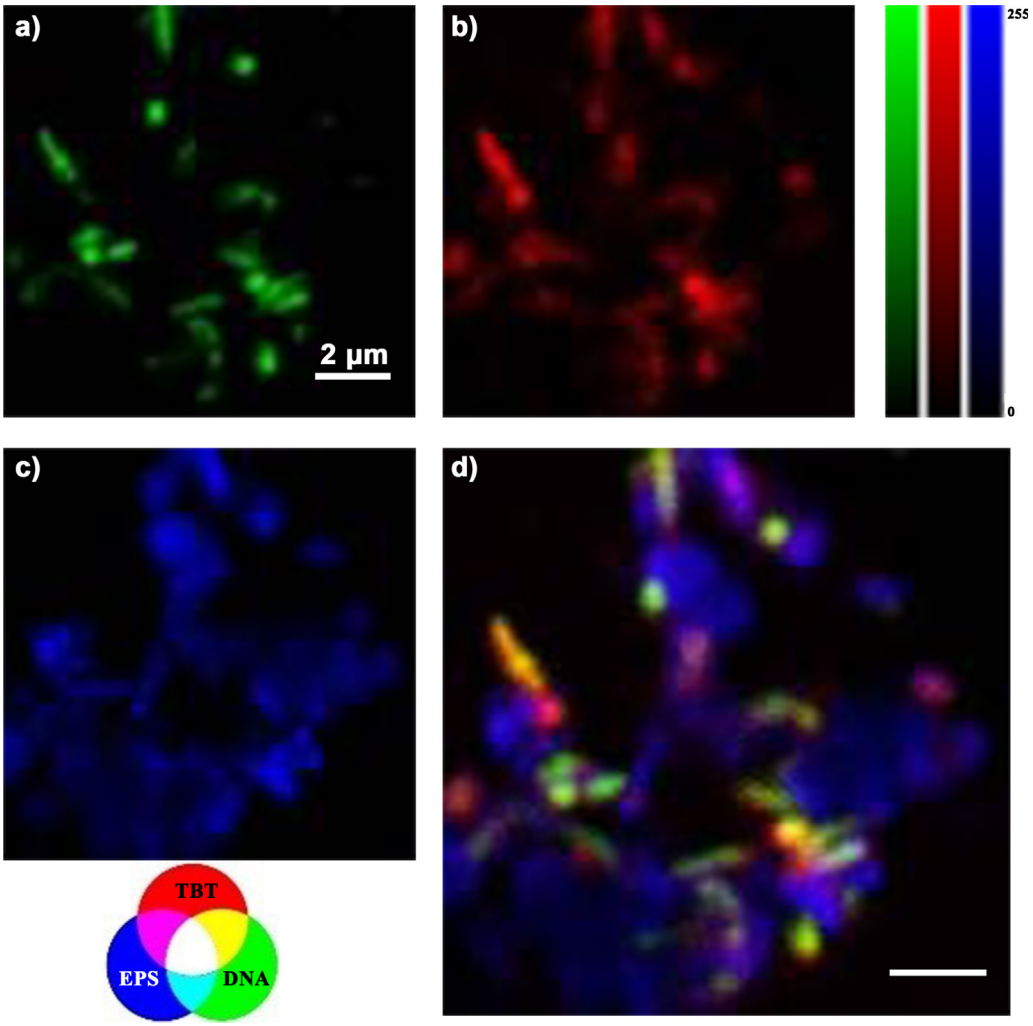

Fig. 5. Single cell scale maps of the sorption of TBT to cell-EPS-mineral aggregates formed by the phototrophic Fe(II)-oxidizing *Rhodobacter* sp. strain SW2 incubated with 50 μM TBT for 1 h at 25 °C. The aggregate was simultaneously incubated with 50 μM probe **1a** (b), fluorescent nucleic acid stain (a) and lectin conjugate (c) for 1 h at 25 °C. (λ_{ex} = 488 nm, 561 nm, 635 nm). The overlay image of (a–c) is shown in (d). Scalebar 2 μm.

optical spectra of the other probes are shown in the Supporting information.

The fluorescence titration of TBT to probe **1a** (5 μM) was conducted in CH_3CN–PBS (1/99, v/v, pH 7.4) solution. As shown in Fig. 2, the TBT-free probe **1a** showed almost no fluorescence. However, the addition of TBT induced significant changes in the fluorescence spectra with an intense fluorescence emission peak at 577 nm, and up to a 202-fold enhancement in fluorescence intensity. About 5.0 equiv. of TBT were required for saturating the fluorescence intensity under the chosen conditions. The intense absorption peak at 556 nm in the absorption spectra of probe **1a** upon the addition of TBT is in good agreement with the fluorescence intensity enhancement (Fig. 1). A good linear relationship between the fluorescence intensity/absorption and the concentration of TBT was obtained for a wide concentration range from 6 to 20 μM of TBT (Fig. 1). 250 nM of TBT was observed to be the detection limit (S/N = 3) of probe **1a**.

To confirm the selectivity of probe **1a**, related transition and main group metal ions were tested under the same conditions. As shown in Fig. 2, no significant fluorescent or absorptive changes were found in the presence or absence of 10 μM TBT with metal ions (30 μM) such as Ni^{2+}, Cd^{2+}, Hg^{2+}, Mn^{2+}, Pb^{2+}, Ca^{2+}, Ba^{2+}, Fe^{3+}, Mg^{2+}, Na^{+}, K^{+}, Co^{2+}, Ag^{+}, Fe^{2+}, Zn^{2+}, Cr^{3+}, Cu^{2+}. Only the presence of TBT resulted in a remarkable enhancement of fluorescence at 577 nm (absorbance at 558 nm). To evaluate the selectivity of the probe for TBT in marine environments, the fluorescence properties of probe **1a** were examined in the presence of other butyltin derivatives and tin. Notably, most of them did not lead to any fluorescence intensity fluctuation. Only monobutyltin and dibutyiltin triggered a small fluorescene enhancement and have nearly no interference to TBT detection (Fig. 3). Moreover, a similar response was observed when TBT was added to the probe solution in the presence of related ions.

Additionally, we determined the effect of pH on the fluorescence response of probe **1a** to TBT (Fig. S1). Without TBT, no obvious characteristic absorption or fluorescence could be observed for probe **1a** between pH 5.0–8.0. Upon addition of TBT, probe **1a** responds stably to TBT within this pH range and we did not observe any interference by protons. Thus, we conclude that probe **1a** has optimal sensing response at physiological pH suggesting that the probe could be promising for biological applications.

Job's plot analyses were used to determine the stoichiometry between probe **1a** and TBT. The 1:1 stoichiometry is the most probable binding mode of probe **1a** and TBT according to a maximum absorbance at 558 nm when the molecular fraction of probe **1a** was close to 50% (Figs. S2 and 3). The mass spectrum manifested a peak at *m*/*z* 879.3826 (Fig. S100), which was assigned as $[\mathbf{1a} + Sn(n\text{-butyl})_3]^+$, providing further evidence for the proposed binding mode. To examine whether the process is reversible, an

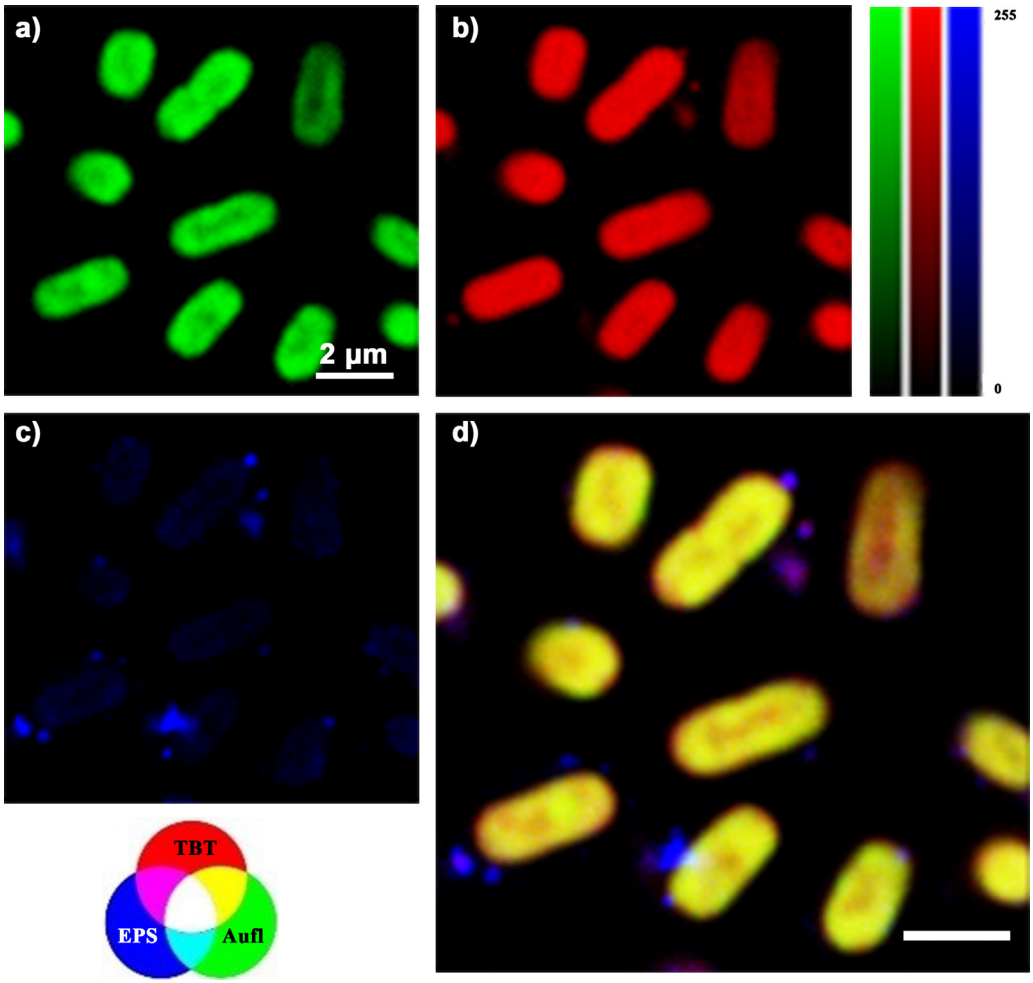

Fig. 6. Single cell scale maps the localization of TBT in marine cyanobacterium *Synechococcus* PCC 7002 incubated with 50 μM TBT for 1 h at 25 °C. Subsequently, the bacterial cells were simultaneously incubated with 50 μM of probe **1a** (b) and lectin conjugate (c) for 1 h at 25 °C. (a) Shows the autofluorescence of the cells. (λ_{ex} = 635 nm, 561 nm, 488 nm). The overlay (d) of the previous imges (a–c) allows for the identification of the colocalizations of TBT with the constituents of the biofilm.

excess amount of EDTA was added into the solution of probe **1a** that was pre-incubated with TBT. The bright fluorescence immediately turned off and the pink color of the solution disappeared (Figs. S4 and 5). This result implies reversible binding of probe **1a** with TBT (Scheme 2).

One of the most important and useful practical applications of probe **1a** is to detect TBT in environmental samples and under environmentally relevant geochemical conditions. We therefore tested probe **1a** for the detection of TBT in artificial seawater. The selected water samples were analyzed without and with the addition of TBT (Fig. S7). Without addition of TBT, no significant fluorescence responses were found. Only the addition of TBT (15 μM) resulted in a significant enhancement of fluorescence in each case. This result indicates that probe **1a** can detect TBT in natural water samples, which are more complex in composition compared to laboratory conditions.

3.2. Density functional theory (DFT) calculations

In order to understand the mechanism of reaction better, DFT [23] calculations based on the Fukui function $f^+(r)$ [23] (Eq. (1)) are performed for the probe with PBE0 functional [24]. Basis set of double-ζ quality (6-31G** for C, H elements, 6-31 + G* for O, N elements) is used for the geometry optimization and the following single point energy calculation. The optimized structure is proven to be the local minimum based on the results of vibration analysis (Scheme 3). All the calculations are performed with the Gaussian 03 program [25].

$f^+(r)$ has been successfully used to describe the reactivity concerning nucleophilic attack [26], such as the mechanism of TBT detection in the present study. According to NBO analysis [27], the condensed Fukui function (Fig. 4) of imidecarbonyl O (1a: 0.103; 1b: 0.117; 1c: 0.039), enamine N (**1a**: 0.065; **1b**: 0.082; **1c**: 0.077) were larger than that of amide N (**1a**: −0.001; **1b**: −0.013; **1c**: −0.001), which indicates that the imidecarbonyl O and enamine N should be the better active site to bind with TBT.

3.3. Fluorescence images

A preliminary study was performed to test the potential application of probe **1a** for high-throughput screenings for the identification of TBT resistant and TBT degrading bacteria. Probe **1a** was applied to visualize TBT in microbial aggregates by confocal laser scanning microscopy. Freshwater photosynthetic Fe(II)-oxidizing *Rhodobacter* sp. strain SW2 (Fig. 5) and marine cyanobacterium *Synechococcus* PCC 7002 were selected and incubated in fresh water mineral and artificial sea water medium, respectively, with light for 1 week, before TBT was added. To localize the TBT in microbial aggregates, DNA- and polysaccharide-specific fluorescent dyes [28] (such as Syto® dyes and lectin-Alexa Fluor® conjugates) were applied simultaneously with probe **1a**. For *Rhodobacter* sp. strain SW2, the fluorescence signal of probe **1a**

indicates that TBT is co-located with both the cells and the free, cloud-like EPS. In contrast, for *Synechococcus* PCC 7002 (Fig. 6), where capsule-like EPS structures enclose the cell, the overlay images indicated that high concentrations of TBT are located within the cell "envelope" structures. This may provide binding sites for TBT and thus might be used to remove TBT from contaminated aqueous environments. Our results indicate that probe **1a** can be used to visualize TBT in living microbial aggregates under natural, hydrated conditions to avoid artifacts from sample preparation. Additionally, this novel probe provides new possibilities to study the TBT antifouling mechanism in both static and dynamic situations. Finally, probe **1a** provides a possible tool for the analysis of microbial TBT resistance, biosorption and biodegradation.

4. Conclusions

From our study we summarize and conclude that six novel rhodamine-based fluorescence probes for TBT were designed, synthesized and tested demonstrating high selectivity and sensitivity with a linear detection range from 6 to 20 μM of TBT. One probe was successfully used to map TBT sorption in cell-EPS-mineral aggregates formed by the *Rhodobacter* sp. strain SW2 and by the marine cyanobacterium *Synechococcus* PCC 7002 by confocal laser scanning microscopy. This approach could be a powerful tool to selectively screen native bacterial strains and environmental microbial biofilms for efficient removal of TBT from contaminated aqueous environments.

Acknowledgements

This work was supported by the NSF of China (No. 21272184,20972124, 21143010, 21103137), the NSF of Shannxi Provincial (No. 2012JQ2007), the Project of Experimental Teaching Research of Northwest University (No. 20120013) and the Emmy-Noether fellowship program of the DFG to M.O. (OB 362/1-1). B. Yin wants to express his thanks to Prof. Yuanhe Huang (College of Chemistry, Beijing Normal University) for his great help.

Appendix A. Supplementary data

Supplementary data associated with this article can be found, in the online version, at http://dx.doi.org/10.1016/j.aca.2014.10.005.

References

[1] T.D. Jickells, Science 281 (1998) 217–222.
[2] S.P. Wilson, Nature 455 (2008) 1029.
[3] R. Costanza, R. d'Arge, R. De Groot, S. Farber, M. Grasso, B. Hannon, Nature 387 (1997) 253–260.
[4] H.K. Okoro, O.S. Fatoki, F.A. Adekola, B.J. Ximba, R.G. Snyman, Asian J. Chem. 23 (2011) 473–482.
[5] A. Adeeko, D. Li, D.S. Forsyth, V. Casey, G.M. Cooke, J. Barthelemy, D.G. Cyr, J.M. Trasler, B. Robaire, B.F. Hales, Toxicol. Sci. 74 (2003) 407–415.
[6] S. Wuertz, C.E. Miller, R.M. Pfister, J.J. Cooney, Appl. Environ. Microbiol. 57 (1991) 2783–2789.
[7] S. Lee, J. Chung, H. Won, D. Lee, Y.-W. Lee, Bull. Environ. Contam. Toxicol. 88 (2012) 239–244.
[8] J.S. White, J.M. Tobin, J.J. Cooney, Can. J. Microbiol. 45 (1999) 541–554.
[9] J. Du, M. Hu, J. Fan, X. Peng, Chem. Soc. Rev. 41 (2012) 4511–4535.
[10] Y. Yang, Q. Zhao, W. Feng, F. Li, Chem. Rev. 113 (2012) 192–270.
[11] M. Schäferling, Angew. Chem. Int. Ed. 51 (2012) 3532–3554.
[12] H.N. Kim, W.X. Ren, J.S. Kim, J. Yoon, Chem. Soc. Rev. 41 (2012) 3210–3244.
[13] S.K. Sahoo, D. Sharma, R.K. Bera, G. Crisponi, J.F. Callan, Chem. Soc. Rev. 41 (2012) 7195–7227.
[14] J. Kovács, T. Rödler, A. Mokhir, Angew. Chem. Int. Ed. 45 (2006) 7815–7817.
[15] W. Domaille, L. Zeng, C.J. Chang, J. Am. Chem. Soc. 132 (2010) 1194–1195.
[16] A. Zhu, Q. Qu, X. Shao, B. Kong, Y. Tian, Angew. Chem. 124 (2012) 7297–7301.
[17] G. Masanta, C.S. Lim, H.J. Kim, J.H. Han, H.M. Kim, B.R. Cho, J. Am. Chem. Soc. 133 (2011) 5698–5700.
[18] H.M. Kim, M.S. Seo, M.J. An, J.H. Hong, Y.S. Tian, J.H. Choi, O. Kwon, K.J. Lee, B.R. Cho, Angew. Chem. Int. Ed. 47 (2008) 5167–5170.
[19] X. Zhang, Y. Xiao, X. Qian, Angew. Chem. Int. Ed. 47 (2008) 8025–8029.
[20] S.-K. Ko, Y.-K. Yang, J. Tae, I. Shin, J. Am. Chem. Soc. 128 (2006) 14150–14155.
[21] A. Kappler, D.K. Newman, Geochim. Cosmochim. Acta 68 (2004) 1217–1226.
[22] X. Jin, L. Hao, Y. Hu, M. She, Y. Shi, M. Obst, J. Li, Z. Shi, Sens. Actuators B 186 (2013) 56–60.
[23] W. Parr, R.G. Yang, Density Functional Theory of Atoms and Molecules, Oxford University Press, New York, 1989.
[24] J.P. Perdew, K. Burke, Phys. Rev. Lett. 77 (1996) 3865–3868.
[25] Gaussian 03, M.J. Frisch, G.W. Trucks, H.B. Schlegel, G.E. Scuseria, M.A. Robb, J. R. Cheeseman, J.A. Montgomery Jr., T. Vreven, K.N. Kudin, J.C. Burant, J.M. Millam, S.S. Iyengar, J. Tomasi, V. Barone, B. Mennucci, M. Cossi, G. Scalmani, N. Rega, G.A. Petersson, H. Nakatsuji, M. Hada, M. Ehara, K. Toyota, R. Fukuda, J. Hasegawa, M. Ishida, T. Nakajima, Y. Honda, O. Kitao, H. Nakai, M. Klene, X. Li, J. E. Knox, H.P. Hratchian, J.B. Cross, C. Adamo, J. Jaramillo, R. Gomperts, R.E. Stratmann, O. Yazyev, A.J. Austin, R. Cammi, C. Pomelli, J.W. Ochterski, P.Y. Ayala, K. Morokuma, G.A. Voth, P. Salvador, J.J. Dannenberg, V.G. Zakrzewski, S. Dapprich, A.D. Daniels, M.C. Strain, O. Farkas, D.K. Malick, A.D. Rabuck, K. Raghavachari, J.B. Foresman, J.V. Ortiz, Q. Cui A.G. Baboul, S. Clifford, J. Cioslowski, B.B. Stefanov, G. Liu, A. Liashenko, P. Piskorz, I. Komaromi, R.L. Martin, D.J. Fox, T. Keith, M.A. Al-Laham, C.Y. Peng, A. Nanayakkara, M. Challacombe, P.M.W. Gill, B. Johnson, W. Chen, M.W. Wong, C. Gonzalez, J.A. Pople, Gaussian, Inc., Pittsburgh PA, 2003.
[26] D. Qi, L. Zhang, L. Zhao, X. Cai, J. Jiang, ChemPhysChem 13 (2012) 2046–2050.
[27] A.E. Reed, L.A. Curtiss, F. Weinhold, Chem. Rev. 88 (1988) 899–926.
[28] B. Zippel, T.R. Neu, Appl. Environ. Microbiol. 77 (2011) 505–516.